# Structure of the Antimicrobial, Cationic Hexapeptide Cyclo(RRWWRF) and Its Analogues in Solution and Bound to Detergent Micelles

Christian Appelt, Axel Wessolowski, J. Arvid Söderhäll, Margitta Dathe, and Peter Schmieder*[a]

*Antimicrobial, cationic peptides are abundant throughout nature as part of many organisms' defence against microorganisms. They exhibit a large variety of sequences and structural motifs and are thought to act by rupturing the bacterial membrane. Several models based on biophysical experiments have been proposed for their mechanism of action. Here we present the NMR-determined structure of the cyclic, cationic antimicrobial peptide cyclo(RRWWRF) both free in aqueous solution and bound to detergent micelles. The peptide has a rather flexible but ordered structure in water. A distinct structure is formed when the peptide is bound to a detergent micelle. The structures in neutral and negatively charged micelles are nearly identical but differ from that in aqueous solution. The orientation of the amino acid side chains creates an amphipathic molecule with the peptide backbone forming the hydrophilic part. The orientation of the peptide in the micelle was determined by using NOEs and paramagnetic agents. The peptide is oriented mainly parallel to the micelle surface in both detergents. Substitution of the arginine and tryptophan residues is known to influence the antimicrobial activity. Therefore the structure of the micelle-bound analogues cyclo(RRYYRF), cyclo(KKWWKF) and cyclo(RRNalNalRF) were also determined. They exhibit remarkable similarities in backbone conformation and side-chain orientation. The structure of these peptides allows the side-chain properties to be correlated to biological activity.*

## Introduction

Antimicrobial peptides are part of the natural immune system of many living organisms.[1] They are either stored in granules or vesicles and excreted rapidly or they can be synthesized quickly. A broad range of microorganisms, which include Gram-positive and negative bacteria and fungi, are affected by these peptides that are evolutionary ancient weapons. Usually a cocktail of multiple peptides is present to supplement the pathogen-specific immune response, which occurs relatively slowly. As bacterial resistance to existing antibiotics grows constantly, these peptides generate interest because they have the potential to form an entirely new drug generation.[2]

Usually, the peptides are expressed in form of larger precursors that are subsequently tailored with a variety of post-translational modifications. These modifications include proteolytic digestion, carboxy-terminal amidation and cyclization either in a head-to-tail fashion or by cystine bridges.[1] The sequences of antimicrobial peptides exhibit a large diversity as do the conformations determined so far.[3,4] Common to the majority of the peptides is their usually positive charge at neutral pH and their amphipathic design in which hydrophobic and cationic residues are organized in different parts of the molecule.

Despite a growing interest in these types of peptides, their mechanism of action is largely unknown. Since replacement of L-amino acids with their D-enantiomers does not in many cases destroy the antimicrobial activity of the peptides—unless the overall structure is disrupted—a mechanism that involves a specific receptor is unlikely.[5] Therefore, it has been proposed that the bacterial membrane might be the target of the antimicrobial assault. The outer membranes of Gram-positive and negative bacteria are negatively charged; they mainly consist of phosphatidylglycerol or lipopolysaccharide, respectively. In contrast, the outer membrane of the mammalian cell mostly contains phosphatidylcholine and is neutral at physiological pH. It is assumed that the negative charge is responsible for the selectivity. Several models have been proposed to explain a membrane-rupture mechanism based on evidence from several biophysical methods.[6–8] Most of the models have been derived based on abundant data from amphipathic helical peptides. Given the variety of bacterial membrane compositions and the diversity of antimicrobial peptides, however, their action does not necessarily have to depend on a single mechanism. Furthermore, it has been shown for some of these peptides that they fail to depolarize the bacterial cytoplasmic membrane at their minimal inhibitory concentration.[9] Therefore, cytoplasmic targets such as DNA also have to be considered.[10,11] Nevertheless, to reach any intracellular target, the peptides have to interact with the membrane in a way that enables the translocation of the usually charged molecules. Membrane interactions are therefore studied here in order to understand the peptides' mechanism of action.

[a] *C. Appelt, Dr. A. Wessolowski, Dr. J. A. Söderhäll, Dr. M. Dathe, Dr. P. Schmieder*
*Forschungsinstitut für Molekulare Pharmakologie*
*Robert-Rössle-Straße 10, 13125 Berlin (Germany)*
*Fax: (+49) 30-94793-230*
*E-mail: schmieder@fmp-berlin.de*

  DOI: 10.1002/cbic.200500095 

The class of the arginine- and tryptophan-rich peptides have also been subject to structural studies.[12–15] Some of these peptides are highly active despite very short sequences.[5,16–18] It is of particular interest to elucidate their mechanism of action since they are too short to span a membrane and a pore formation seems unlikely. However only little structural information is available for such small peptides.[19,20] The linear peptide Ac-RRWWRF-$NH_2$, originally discovered from a synthetic combinatorial library,[18] shows a high sequence similarity to core fragments of some naturally occurring antimicrobial peptides.[5] Backbone cyclization of the linear peptide reduces the minimum inhibitory concentration tenfold, possibly by restricting the conformation to a highly active structure.[17]

Here we present the structure of the cyclic hexapeptide cyclo(RRWWRF), or c-RW, as determined by NMR spectroscopy. Experiments were carried out in aqueous solution, negatively charged sodium dodecyl sulphate (SDS) and neutral dodecylphosphocholine (DPC) micelles that mimic a membrane environment. Relaxation agents were used in addition to NOE data to elucidate the orientation of the peptides in the micelles.

Substitution of the arginines by lysines reduces the activity as does the replacement of tryptophans by tyrosines. An increase in antimicrobial properties is caused by replacing the tryptophans by β-(2-naphtyl)-L-alanine.[5] We investigated the DPC-micelle-bound structure of the peptides c-RY (cyclo(RRYYRF)), c-KW (cyclo(KKWWKF)) and c-RNal (cyclo(RRNalNalRF)) to understand the changes in activity that are due to substitution of arginine and tryptophan residues.

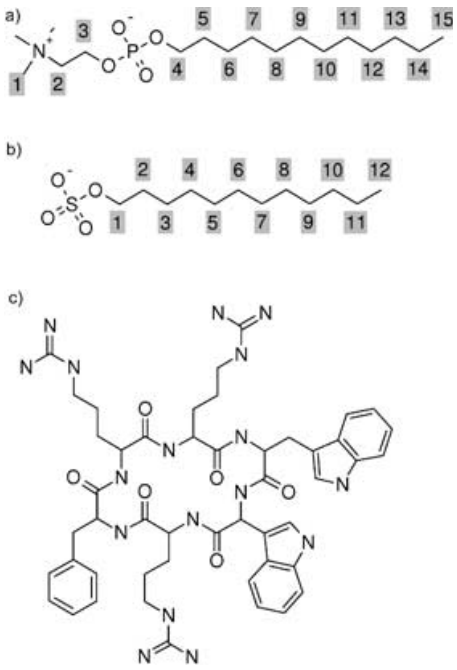

**Scheme 1.** Chemical formulae of a) DPC and b) SDS showing the numbering scheme of protons. c) Chemical formula of c-RW.

## Results

### NMR spectroscopy

The structure of c-RW was determined in three different environments: in aqueous solution and in the presence of SDS and DPC detergent micelles (Scheme 1). The concentration of c-RW (2.5 mM) was constant in all investigations. The concentrations for SDS (25 mM) and DPC (50 mM) resulted in a peptide-to-lipid ratio of 1:10 and 1:20, respectively. In all three environments, the peptide showed a good dispersion of signals from amide protons in 1D $^1$H NMR spectra (data not shown); this indicates an ordered structure. Notably, c-RW did not show any NOE effects at 600 MHz in aqueous solution. To obtain distance information the ROESY technique had to be used (Figure 1a). This made sure that NOE information extracted from NOESY spectra in the presence of detergent micelles (Figure 1b and c) originated exclusively from micelle-bound peptides. Besides 2D NOESY and ROESY spectra a set of 2D TOCSY spectra were recorded along with a DQF-COSY. For the determination of $H^N$,$H^\alpha$ coupling constants an in-phase COSY spectrum based on the HNHA experiment was used (see Experimental Section). No heteronuclear techniques were used since the concentration of the peptide was too low. All spectra were recorded at 300 K. For peptides c-RY, c-RNal and c-KW the same set of spectra were recorded in the presence of DPC micelles under identical conditions. Resonance assignment was achieved by using a conventional sequence specific assignment based on NOESY or ROESY and TOCSY spectra.[21] Spin systems were identified in TOCSY spectra and subsequently linked with $H^\alpha_i$,$H^N_{i+1}$ (sequential) cross-peaks in the NOESY or ROESY spectra. Side-chain assignments were confirmed by using the DQF-COSY. Aromatic resonances were assigned by using a combination of TOCSY and DQF-COSY and NOE cross-peaks between resonances of aromatic protons and those of other side-chain protons. A complete assignment of all proton resonances could be obtained that way for c-RW under all three solvent conditions and for c-RY and c-KW bound to DPC micelles. The assignment of the aromatic protons of the c-RNal naphthylalanine was incomplete due to signal overlap. Since chemical shift is a sensitive indicator of structure, the assignment indicated that the structure of the c-RW peptide in aqueous solution was different from that bound to detergent micelles. The assignments were similar for both detergents. The DPC-micelle-bound analogues of c-RW showed similar resonance patterns; this suggests a conserved structure.

### Structure determination of c-RW

The structure of c-RW was based on distances from NOE or ROE intensities and angles from homonuclear coupling constants.

Not unexpectedly for a cyclic hexapeptide in aqueous solution, c-RW turned out to be rather flexible. The number of ROEs was not high but was sufficient to define an ordered structure (Figure 2a). It resembles the combination of two β-turns. Amino acids R1 to W4 form one turn with R2 and W3 in the *i*+1 and *i*+2 position, respectively; amino acids W4 to R1 form the other turn with R5 and F6 in the *i*+1 and *i*+2 posi-

  

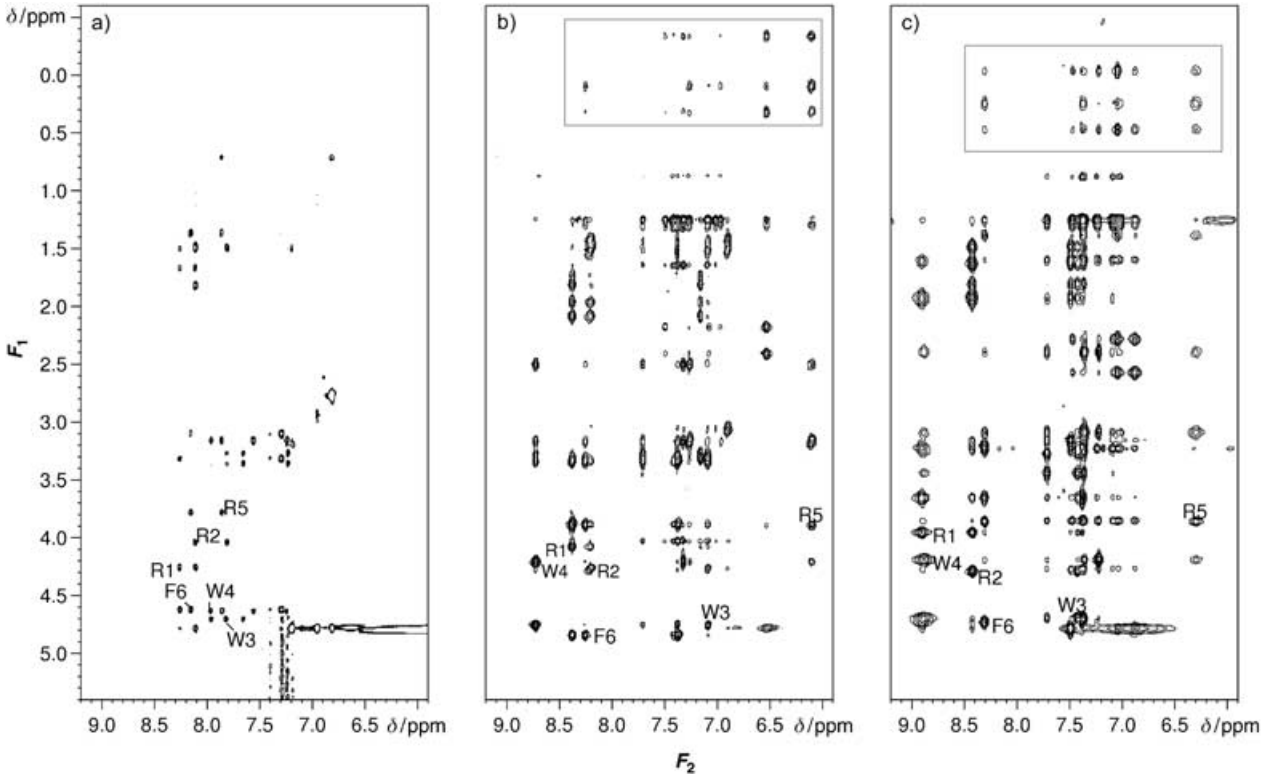


**Figure 1.** Representative section of the 80 ms ROESY spectrum of c-RW (2.5 mM) in water a) acquired at 600 MHz. The same region of the 80 ms NOESY spectra of c-RW (2.5 mM) in b) SDS (25 mM) and c) DPC (50 mM). The grey rectangles mark cross peaks between aromatic side chains and R5 β- and γ-protons. This exemplifies distinct side chain conformations. The unusual up-field shift of the R5 protons, which is due to close contact with the aromatic residues, is also worth noting.

tions, respectively. The region of the amino protons in the ROESY spectrum is shown in Figure 1a.

The structure changes quite dramatically when c-RW is bound to SDS. It still consists of two β-turns but the position of the turns in the sequence shifts. This results in a root mean square deviation (RMSD) of 3.6 Å for the heavy atoms of the average structures. The region of the amide-proton resonances in the NOESY spectrum is shown in Figure 1b. The number of NOEs has increased drastically compared to the structure in water (Table 1). In particular NOEs between protons of the amino acid side chains allow for a much better definition of the side-chain structures. This is shown by the example of R5 cross signals to the aromatic protons (grey rectangle in Figure 1b). This residue is in close contact with the aromatic amino acids and causes a strong up-field shift of almost 2 ppm for the β and γ protons. The structure is shown in Figure 2b. It exhibits a βI turn from F6 to W3 and a βII′ turn from W3 to F6. The aromatic residues are clustered on one side of the molecule.

When bound to DPC micelles, the structure of c-RW was found to be quite similar to the one in SDS, with a heavy atom RMSD of 1.7 Å for the average structures. This is already visible from the NOESY spectrum (Figure 1c); only small differences are detectable between the two spectra with respect to the peptide signals. Again the pattern of NOE signals from the R5 side-chain protons to the aromatic protons (grey rectangle in Figure 1c) exemplifies the well defined side-chain conformation. The structure is shown in Figure 3a and a superposition of the structures determined in the two different micelle environments is shown in Figure 3b. As in SDS, all aromatic side chains point towards one side of the peptide while the other side is formed by the backbone. This creates an amphipathic molecule. Figure 4 shows a hydrophobicity map of the surface of c-RW in DPC micelles. The hydrophobic face is formed by the side chains of the aromatic residues, the backbone on the opposite side forms the hydrophilic part.

### Structure of c-RY, c-KW and c-RNal

There were also remarkable similarities between the structures of DPC-bound c-RY (Figure 5a) and c-KW (Figure 5b) when compared with the micelle-bound c-RW. In both cases the backbone formed a βI turn from residue six to residue three. A βII′ turn stretched from residue three to residue six. A comparable orientation of the side chains was observed to result in an amphipathic structure for both molecules. The RMSD between the identical heavy atoms of the average structures was 0.96 Å for c-KW to DPC-bound c-RW and 1.59 Å for c-RY to DPC-bound c-RW.

The calculated ensemble of DPC-bound c-RNal (Figure 5c) was less well but still sufficiently defined due to incomplete resonance assignment. The backbone conformation was different from the previous structures in that its β-turns cannot be grouped into defined categories anymore. However, the side

  

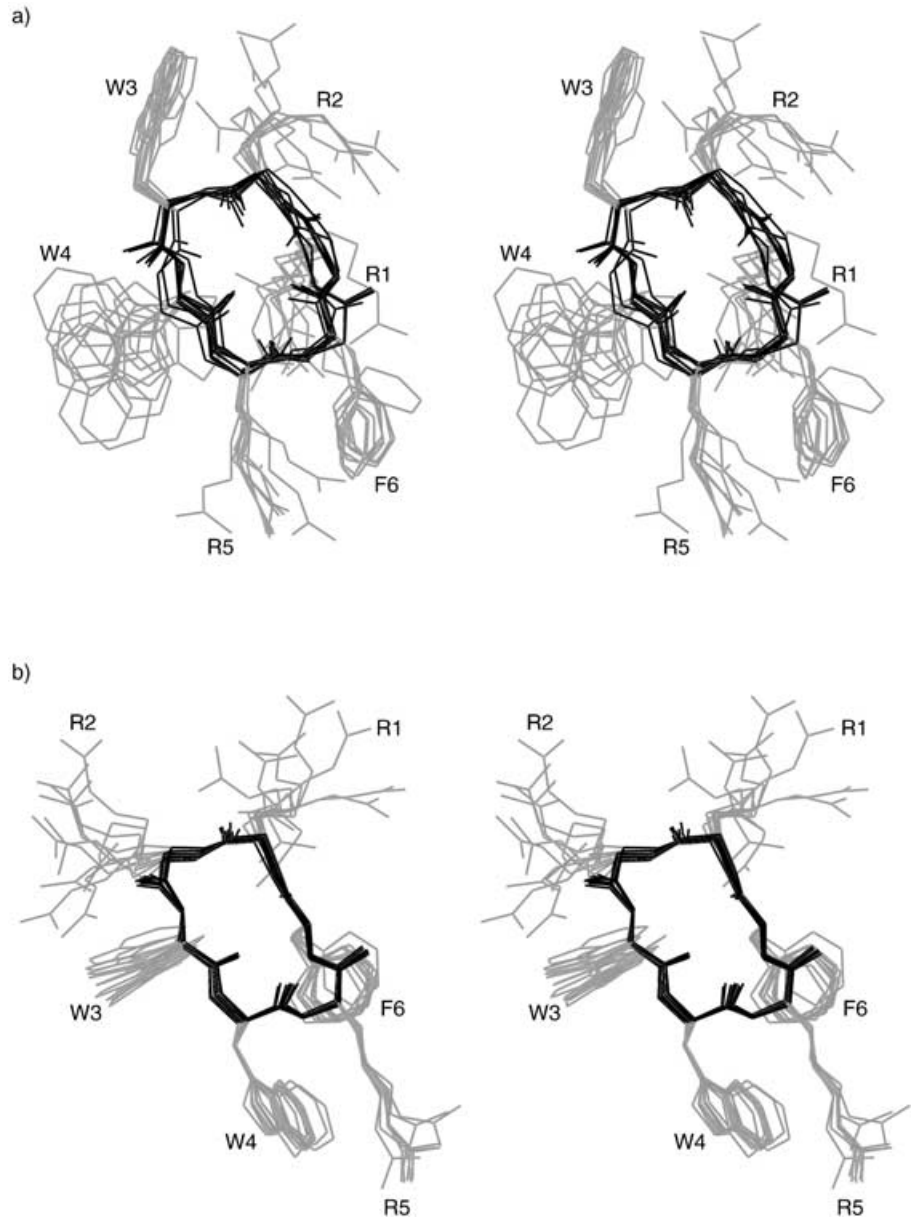


**Figure 2.** Overlay of the ten lowest energy conformers of c-RW a) in water and b) bound to SDS micelles.

**Table 1.** Restraints used in the simulated annealing, violations and RMSDs for each structure.

| | c-RW/$H_2O$ | c-RW/SDS | c-RW/DPC | c-RY | c-KW | c-RNal |
|---|---|---|---|---|---|---|
| **Distance restraints** | | | | | | |
| total | 57 | 136 | 125 | 124 | 168 | 103 |
| intraresidue | 40 | 65 | 65 | 64 | 82 | 37 |
| sequential | 17 | 55 | 52 | 43 | 69 | 50 |
| medium range | 0 | 16 | 8 | 17 | 17 | 16 |
| dihedral restraints | 0 | 5 | 4 | 3 | 5 | 2 |
| *J*-coupling restraints | 6 | 0 | 2 | 0 | 0 | 0 |
| violations $>$ 0.25 Å | 7 | 0 | 0 | 0 | 0 | 4 |
| **RMSD** | | | | | | |
| backbone in Å | $0.61 \pm 0.20$ | $0.15 \pm 0.06$ | $0.41 \pm 0.13$ | $0.15 \pm 0.07$ | $0.14 \pm 0.10$ | $0.39 \pm 0.14$ |
| heavy atom in Å | $1.90 \pm 0.34$ | $1.38 \pm 0.30$ | $1.94 \pm 0.48$ | $1.66 \pm 0.28$ | $0.60 \pm 0.20$ | $2.08 \pm 0.55$ |
| PDB ID | – | 1QVL | 1QVK | 1SKI | 1SKK | 1SKL |

chains were in a similar orientation to that found in DPC-bound c-RW, with the aromatic side chains and the opposing hydrophilic backbone region forming a distinct amphipathic structure.

To understand the role of the amphipathic structure in determining activity, a lipophilic potential surface was created for each structure. The surface was divided into four classes according to the lipophilic potential (Figure 6). The surface area for each class was calculated as the percentage of the total surface area. SDS- and DPC-micelle-bound c-RW and c-KW showed a balance in the distribution of their hydrophilic/hydrophobic properties. The major part of the surface showed medium hydrophilicity or hydrophobicity. In the case of c-RY by far the largest part of the surface was found to be strongly hydrophilic. A broader distribution was found for c-RNal with areas of medium hydrophilicity and strong hydrophobicity being equally present.

### Orientation of c-RW in the micelle

The information about the orientation of c-RW in the micelles was obtained with relaxation experiments by using a water-soluble, paramagnetic compound, gadolinium diethylenetriaminepentaacetic acid ($Gd^{III}$-DTPA), that was added to the solution.[22] The resulting longitudinal relaxation times ($t_1$) of the peptide protons in presence of $Gd^{III}$-DTPA were compared to those determined in its absence. For protons exposed to the solution and thus to the probe, a strong decrease in $t_1$ can be expected, while protons pointing into the micelle are strongly protected and only a minor effect will be visible. Care was taken to apply $Gd^{III}$-DTPA at a concentration that would not affect the trans-

  

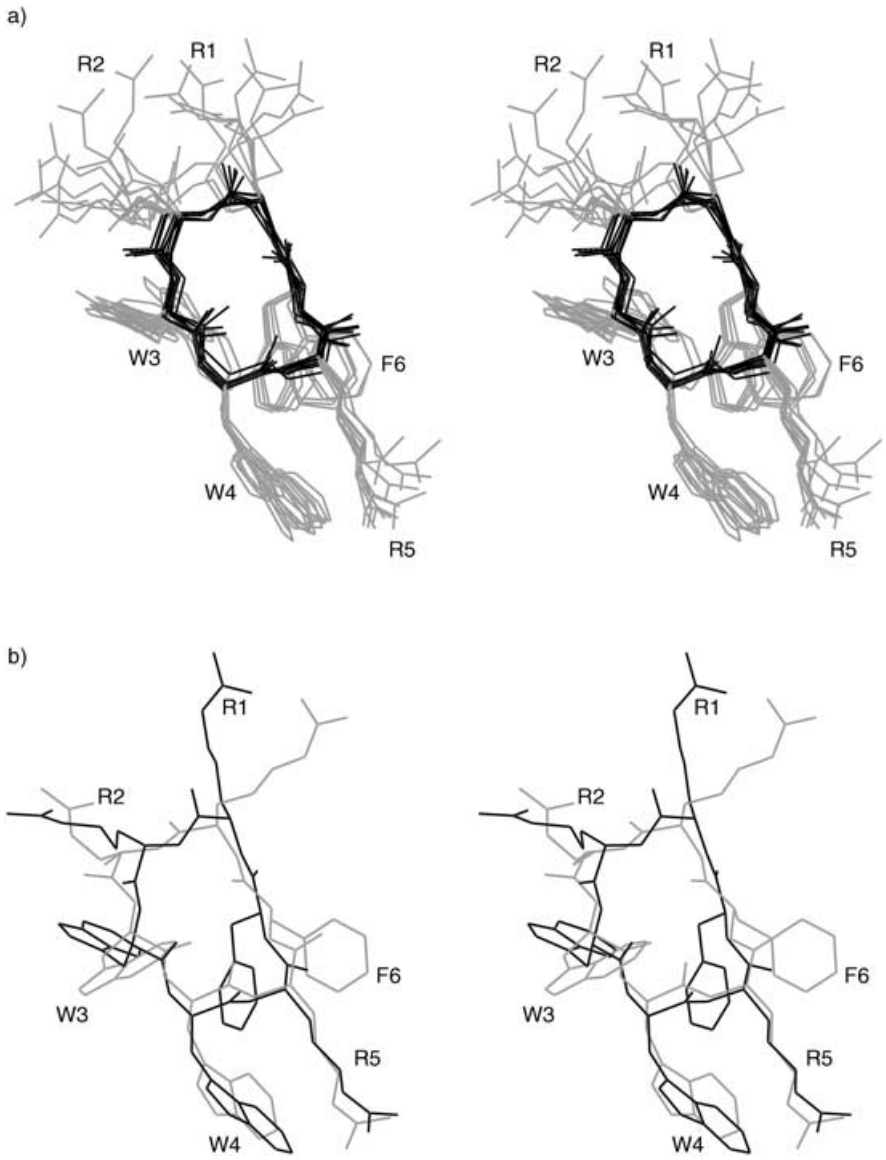


**Figure 3.** a) Overlay of the ten lowest energy conformers of c-RW bound to DPC micelles. b) Superposition of SDS- (grey) and DPC-bound (black) c-RW. For the superposition the structures closest to the average were chosen.

versal relaxation time ($t_2$) too strongly. Thereby, signal overlap of the peptide and detergent protons as a consequence of line broadening was avoided. To obtain a scale for the positioning of c-RW relative to the micelle, the protons of undeuterated detergents were also examined (Figure 7c and d). According to the ratio of $t_1$ in the presence and absence of $Gd^{III}$-DTPA, the protons can be divided into two different classes (Figure 7).

In the case of SDS micelles, the relaxation data indicate that the peptide backbone is oriented parallel to the micelle surface and the amino acid side chains point into the micelle. The aromatic rings exhibit the highest protection from the relaxing agent. This mode of orientation was in agreement with NOEs between protons of the aromatic side chains and protons of the detergent's alkyl chains. Other peptide protons displayed no NOEs to that part of the detergent.

The situation in DPC micelles appears to be slightly different and the molecule seems to be somewhat tilted with respect to the micelle surface. The R1 and R2 side chains exhibit a change in relaxation times. The side chains of the aromatic residues, on the contrary, are more protected against the relaxation probe. Again this orientation could be confirmed through the presence of NOEs between protons of the aromatic side chains and those of the detergent's alkyl chains.

## Discussion

A number of factors are generally considered to be important for the activity of antimicrobial peptides. Among these are the presence of hydrophobic and basic residues and an amphipathic structure.[1] c-RW exhibits these properties. As can be expected for a cyclic hexapeptide, the structure consists of two β-turns and thus represents the smallest possible β-sheet. The structure is, however, not preformed in solution as with several larger β-sheet peptides. The actual position of the amino acids in the two turns of the structure changes from water to detergent. This demonstrates that the structure is in fact strongly influenced by the membrane-mimicking environment and thus difficult to predict from the amino acid composition alone.

The side chains of c-RW turned out to be rather flexible in water, while it showed a well defined side-chain conformation when bound to micelles. This is reflected by a multitude of side-chain-to-side-chain NOEs and unusual chemical shifts for side-chain protons. The latter are due to chemical shift anisotropies induced by the aromatic systems.

The amphipathic structure of c-RW is induced by the lipophilic environment, with a slightly larger hydrophilic and a somewhat smaller hydrophobic surface. However, this amphipathic structure is not formed by the side chains alone. The peptide backbone also contributes to the hydrophilic face of the molecule. The structural investigations have been performed in two different detergent micelles for c-RW, one of them composed of negatively charged lipid molecules and the

  

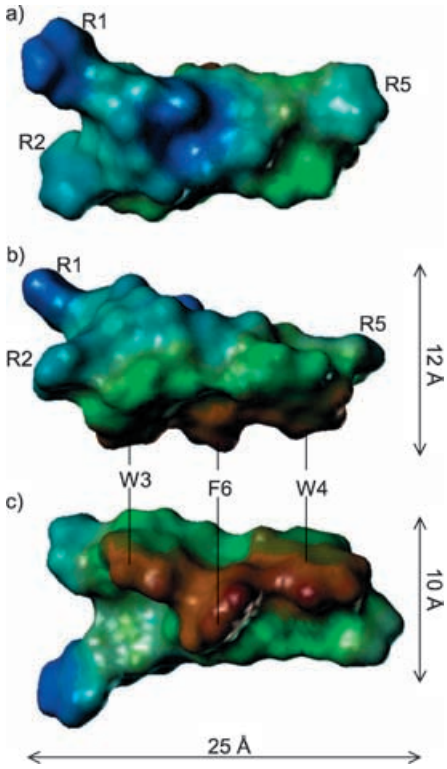


**Figure 4.** Lipophilic potential mapped onto the surface of DPC-bound c-RW. a) View of the backbone, b) side view and c) the aromatic side chains. Brown and blue areas account for hydrophobic and hydrophilic regions, respectively. A distinct amphipathic structure is formed by the clustering of the aromatic side chains opposite the hydrophilic backbone and arginine side chains.

other of zwitterionic molecules. The distribution of charges is also one of the major differences between a bacterial and eukaryotic membrane. This is believed to be of major importance for the mechanism of action of antimicrobial peptides. Interestingly, we find that the structure of the peptide does not differ in the two environments. Even though the structure changes from aqueous solution to a lipid environment, the charge distribution does not affect the structure of the peptide. This is also reflected in previously reported CD spectroscopy data that indicate structural similarities in SDS and palmitoyloleoylphosphatidylcholine (POPC) vesicles.[17] These observations are in contrast to other reports that find differences in structures that are determined in micelles of different charge distributions.[19] The activity of the peptide towards different types of membranes must, at least in the case of c-RW, result from the ability of the membrane to accommodate the peptide. While the overall structure of the peptide itself appears to be independent of the composition of the lipid environment, the interactions between the side chains and the lipids will certainly be affected.

Exposure of the peptide to water was however influenced by the lipid charge, as determined by comparing $t_1$ in the presence and absence of $Gd^{III}$-DTPA. Especially the side chains of R1 and R2 were more water exposed when bound to DPC micelles. This can be attributed to a difference in the electrostatic interactions between peptide and lipids. The SDS head groups bound more tightly to the arginine side chains with only the peptide backbone exposed to the paramagnetic probe. However, the relaxation experiments supported by NOE data could show that the peptide was located at the surface of the micelle in both cases. The cluster of aromatic residues was oriented towards the micelle core and acted as a hydrophobic anchor. This localization is in agreement with other observations that tryptophans within membrane proteins and peptides are preferentially located close to the interface region.[23] The arginine side chains and backbone were located in the lipid-water interface. Thus the arginine side chains have the possibility to interact with the lipid head groups both electrostatically and by hydrogen bonds. This type of interaction has also been described in the literature.[24] We have investigated these interactions by molecular dynamics simulations as described in an accompanying paper.[25]

For the analogues c-RY, c-KW and c-RNal peptides, the structures were determined in the DPC-micelle-bound form. Similar conformations of the backbone and the same orientation of the side chains with clustered aromatic residues gave rise to distinct amphipathic structures. It is not surprising that, for c-RY, the hydrophilic parts dominate; the tyrosine side chains are less bulky and their contribution to the total surface is smaller. The opposite is true for c-RNal since the voluminous naphthylalanine side chains extend to the hydrophobic area. There is a correlation between the hydrophobicity of the structure and erythrocyte lysis with c-RNal: the more hydrophobic analogue is the most effective.[5] The connection with biological activity against *E. coli* and *Bacillus subtilis* is not as obvious (Table 2). Clearly there is a dramatic loss in activity for c-RY when compared to c-RW. On the other hand a gain in activity for c-RNal is species dependent and is of minor importance. This demonstrates that the antimicrobial activity depends on a balanced amphipathicity rather than on a large hydrophobic core. Despite the fact that the size of hydrophilic and hydrophobic areas and the net charge for c-RW and c-KW are comparable, c-KW showed a decreased minimum inhibitory concentration (MIC) and erythrocyte lysis. This can only arise from the difference in the cationic side chain moieties. The guanidino moieties of the arginine side chains possess five H-bond donors, whereas lysine side chains offer only three H-bond donors. Thus the ability to interact with lipid head groups that are abundant in H-bond acceptors is reduced. Also, it has been observed for other peptides that substitution of arginines to lysines decreases their activity.[26]

Several models have been proposed to explain the molecular basis of antimicrobial activity through membrane disruption. The barrel-stave model assumes that the pore is formed by an oligomer of parallel-aligned peptides that span the entire membrane.[27] However, backbone cyclization restricts the maximum possible length of peptide to about 25 Å, from the tip of the R2 side chain to that of the R5. If the hydrophobic core of the membrane were lined by the cluster of aromatic residues, which are only about 16 Å in length, this would result in a considerable hydrophobic mismatch with the membrane, which has a hydrophobic core of approximately 25–30 Å. Since such an arrangement would be highly unfavoura-

  

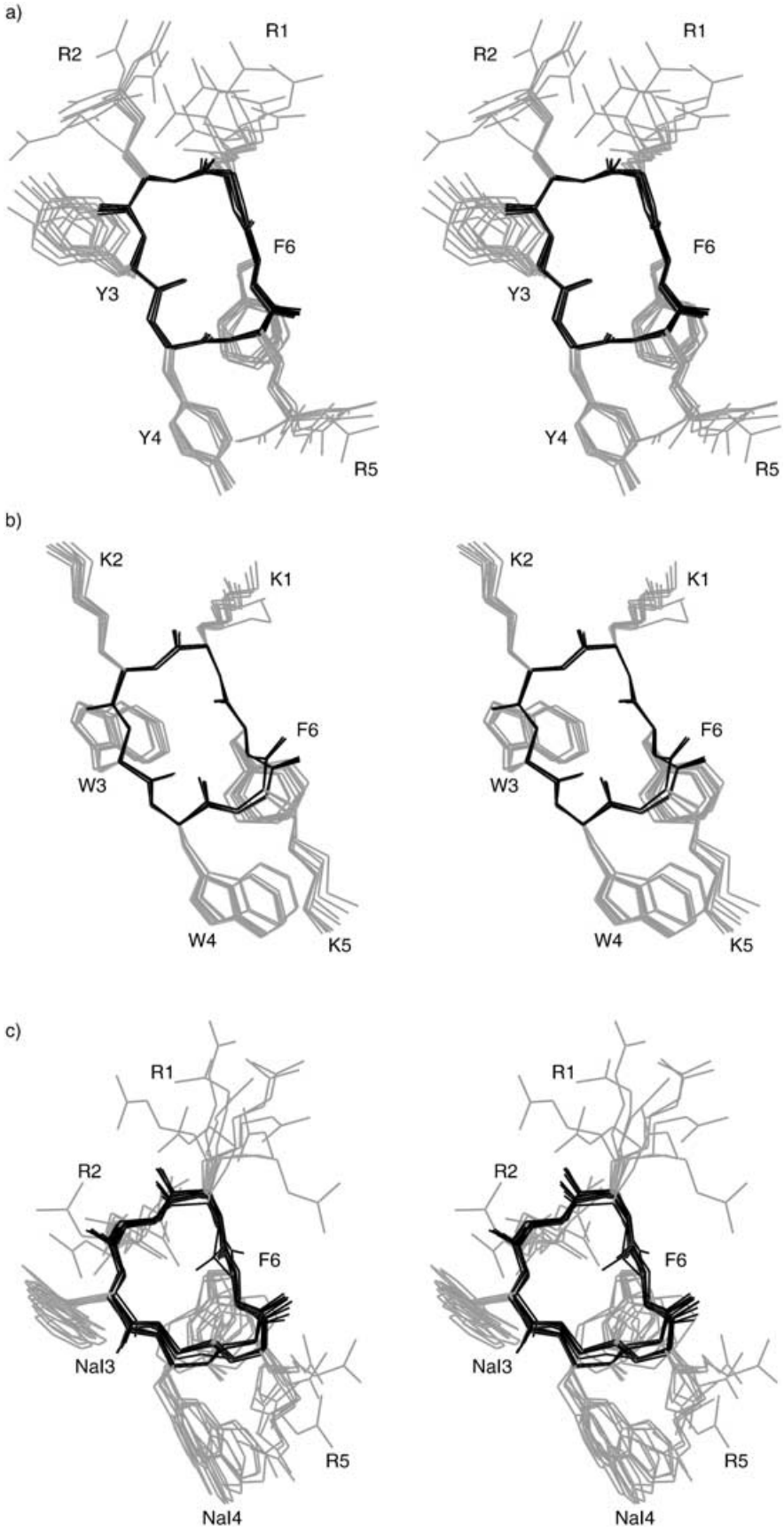


**Figure 5.** Overlay of the ten lowest energy conformers of a) c-RY, b) c-KW and c) c-RNal, all bound to DPC micelles.

ble,[25] it appears that this model cannot be used for the interpretation of the presented results; even though it seems to explain the effect of other helical peptides. Also, for other peptides that could potentially span the membrane in a barrel-stave-like fashion, cyclization makes membrane spanning unlikely without destroying their activity.[28, 29]

The activity therefore, has to be explained by taking a horizontal insertion into account, as determined by NOEs and relaxation experiments. One model that is in agreement with a horizontal insertion is the "carpet model".[6] It describes the binding of peptide monomers to the bilayer surface. When they reach a threshold concentration, the induced curvature strain causes permeation or disintegration of the membrane.

In the model proposed by Matsuzaki the antimicrobial peptide is inserted in the membrane interface and forms supramolecular aggregates with lipid molecules.[7] These aggregates are capable of crossing the membrane barrier, thereby forming transient channels that could facilitate the exchange of ions and larger molecules. The fact that c-RW is more active than c-KW supports this model since arginine chains posses more H-bond donors to form these peptide–lipid aggregates. A more detailed description of a possible mode of action based on a molecular dynamics study of c-RW embedded in a lipid bilayer will be published.[25]

In conclusion we have shown that c-RW undergoes a conformational change upon membrane binding. This results in an altered structure that is induced by the lipid environment, irrespective of the charge. The aromatic residues form a hydrophobic cluster that is anchored in the hydrophobic core of the membrane. The backbone and

  

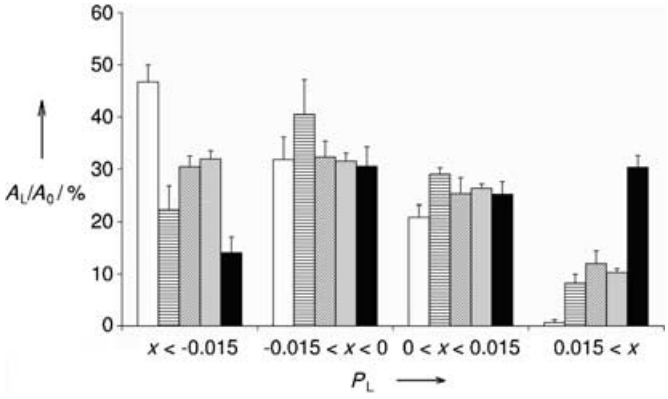


**Figure 6.** Balance of hydrophilic and lipophilic regions. The ratio between the surface area within a certain lipophilic potential ($P_L$) range, $A_L$, and the total surface area, $A_0$, was calculated for c-RY (white), c-RW–SDS (horizontally hatched), c-RW–DPC (diagonally hatched), c-KW (grey) and c-RNal (black). High lipophilic potentials correspond to hydrophobic regions.

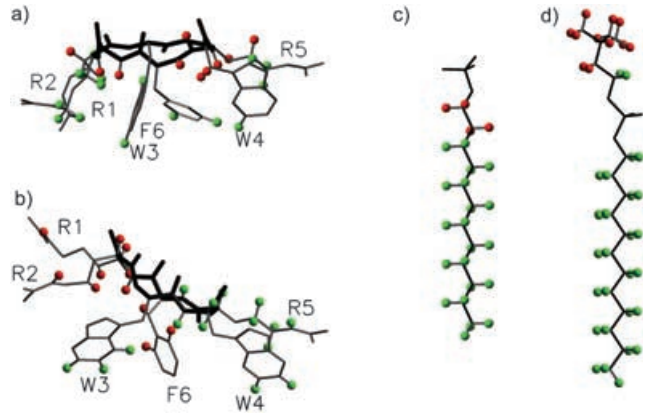


**Figure 7.** Measurement of longitudinal relaxation times of SDS- and DPC-bound c-RW. For protons, $t_1$ in the presence ($t_1^{Gd}$) and absence ($t_1^0$) of $Gd^{III}$-DTPA (0.3 mM) was determined. Red spheres account for $t_1^{Gd}/t_1^0 < 0.6$ (solvent exposed) and green spheres for $t_1^{Gd}/t_1^0 > 0.6$ (less solvent exposed). a) c-RW bound to SDS micelles; b) c-RW bound to DPC micelles; c) SDS with the sulfate pointing upwards; d) DPC with the head group pointing upwards.

the arginine side chains form the hydrophilic face of the molecule and are located at the lipid–water interface. Investigation of the analogues c-RW, c-RY and c-RNal suggests that a balance in amphipathicity is crucial for antimicrobial activity and selectivity. Furthermore, it was shown that lysine side chains are less favourable. This emphasizes a special role for arginine side chains in interacting with the target membrane. The results presented here can exclude a membrane-spanning mode of action.

**Table 2.** Minimal-inhibitory concentration (MIC) and erythrocyte lysis of the investigated peptides.

| | c-RW | c-RY | c-KW | c-RNal |
|---|---|---|---|---|
| sequence | cyclo(RRWWRF) | cyclo(RRYYRF) | cyclo(KKWWKF) | cyclo(RRNalNalRF) |
| MIC *E. coli* [μM] | 6.3 | >100 | 25 | 12.5 |
| MIC *B. subtilis* [μM] | 3.1 | >100 | 25 | 1.6 |
| erythrocyte lysis (100 μM) | 24% | 1% | 10% | >30% |

## Experimental Section

**NMR spectroscopy**: The synthesis of the peptides has been described previously.[5] For the preparation of all samples, c-RW, c-KW, c-RY and c-RNal were dissolved in $H_2O/D_2O$ (9:1, 600 μL; final sample concentration 2.5 mM). To obtain a sample of SDS-micelle-bound peptide (25 mM SDS, pH 4.5) a stock solution of SDS was added. Similarly, protonated (Avanti Polar Lipids, Alabaster, AL, USA) and perdeuterated DPC (Cambridge Isotope Laboratories, Inc., Andover, MA, USA) were applied (50 mM, pH 6.3).

All NMR spectra were recorded on a Bruker DRX600 spectrometer. DQF-COSY,[30] TOCSY (14 ms, 28 ms, 56 ms and 128 ms mixing time),[31] NOESY (mixing time 80 ms),[32] and ROESY (80 ms mixing time)[33] were recorded at 300 K. *J* coupling constants were extracted from an in-phase COSY based on the HNHA experiment.[34,35] Water suppression was achieved by using a WATERGATE sequence.[36] The number of data points in the $F_2$ and $F_1$ dimension was 4096 and 512, respectively. Spectra were multiplied by a squared cosine function and zero-filled to 4 K×2 K by using XWINNMR (Bruker, Karlsruhe, Germany).

To study the water exposure of the peptide when bound to detergent micelles we determined longitudinal relaxation times in the presence and absence of $Gd^{III}$-DTPA.[37] A $Gd^{III}$-DTPA stock solution (50 mM) was prepared by dissolving diethylenetriaminepentaacetic acid (DTPA, 1.02 equiv; Sigma) in NaOH (150 mM) followed by the addition of $Gd^{III}Cl_3$ (1 equiv, Sigma). The stock solution was added to the sample to give a final concentration of 0.3 mM. We recorded a set of 25 1D $^1H$ experiments preceded by a 180° pulse and a relaxation delay ranging from 5 ms to 2 s. For solvent suppression a WATERGATE sequence was applied. Relaxation functions were fitted by using KaleidaGraph 3.51 (Synergy Software, Reading, PA, USA).

**Structure calculation**: The 2D NMR spectra were evaluated by using SPARKY.[38] NOESY cross peaks were fitted with a Gaussian function and interproton distances were derived from the peak volumes. Upper and lower restraint boundaries were obtained by defining a tolerance for the calculated distances of ±0.3 and ±0.7 Å for SDS- and DPC-bound peptide, respectively. Restraint corrections were applied for pseudoatom assignments. Prochiral assignments for β-protons were derived as described by Wagner.[39] Structures were calculated with molecular dynamics simulations by using Amber 6.0.[40] The simulated annealing protocol included an unrestrained high-temperature step for the randomization of the initial structure. Restraints were applied to an additional high-temperature stage. HN-Hα *J* coupling restraints were included directly; the Karplus coefficients were set to $A = 9.5$, $B = -1.4$ and $C = 0.3$.[41] The simulated annealing was concluded by restrained cooling and energy minimization. Out of 100 runs the ten lowest-energy structures were kept as final structures. For structural analysis the program MOLMOL was used.[42] The average of the ten lowest-energy structures was calculated and the one with the lowest RMSD was chosen as the representative structure. The lipophilic potential surfaces were created by using Sybyl 6.9 (Tripos, Inc., St. Louis, MO, USA).

**Deposition in the PDB**: The structures as well as the NMR data have been deposited in the PDB and BMRB. The PDB codes are given in Table 1. Due to its high RMSD, the structure of c-RW in water has not been deposited.

  

## Acknowledgements

*Support of the Forschungsinstitut für Molekulare Pharmakologie (FMP) and from the Deutsche Forschungsgemeinschaft (DA 324/4-1) is gratefully acknowledged. C.A. thanks the Fonds der Chemischen Industrie for a Kekulé fellowship.*

**Keywords:** antimicrobial peptides · membranes · micelles · NMR spectroscopy · peptides

[1] M. Zasloff, *Nature* **2002**, *415*, 389 – 395.
[2] C. Nathan, *Nature* **2004**, *431*, 899 – 902.
[3] R. M. Epand, H. J. Vogel, *Biochim. Biophys. Acta* **1999**, *1462*, 11 – 28.
[4] R. E. Hancock, *Lancet Infect. Dis.* **2001**, *1*, 156 – 164.
[5] A. Wessolowski, M. Bienert, M. Dathe, *J. Pept. Res.* **2004**, *64*, 159 – 169.
[6] Y. Shai, *Biochim. Biophys. Acta* **1999**, *1462*, 55 – 70.
[7] K. Matsuzaki, *Biochim. Biophys. Acta* **1999**, *1462*, 1 – 10.
[8] L. Yang, T. M. Weiss, R. I. Lehrer, H. W. Huang, *Biophys. J.* **2000**, *79*, 2002 – 2009.
[9] M. Wu, E. Maier, R. Benz, R. E. Hancock, *Biochemistry* **1999**, *38*, 7235 – 7242.
[10] H. G. Boman, B. Agerberth, A. Boman, *Infect. Immun.* **1993**, *61*, 2978 – 2984.
[11] C. B. Park, H. S. Kim, S. C. Kim, *Biochem. Biophys. Res. Commun.* **1998**, *244*, 253 – 257.
[12] A. Rozek, C. L. Friedrich, R. E. Hancock, *Biochemistry* **2000**, *39*, 15765 – 15774.
[13] D. J. Schibli, P. M. Hwang, H. J. Vogel, *Biochemistry* **1999**, *38*, 16749 – 16755.
[14] P. M. Hwang, N. Zhou, X. Shan, C. H. Arrowsmith, H. J. Vogel, *Biochemistry* **1998**, *37*, 4288 – 4298.
[15] W. Jing, A. R. Demcoe, H. J. Vogel, *J. Bacteriol.* **2003**, *185*, 4938 – 4947.
[16] M. B. Strom, O. Rekdal, J. S. Svendsen, *J. Pept. Sci.* **2002**, *8*, 431 – 437.
[17] M. Dathe, H. Nikolenko, J. Klose, M. Bienert, *Biochemistry* **2004**, *43*, 9140 – 9150.
[18] S. E. Blondelle, E. Takahashi, K. T. Dinh, R. A. Houghten, *J. Appl. Bacteriol.* **1995**, *78*, 39 – 46.
[19] W. Jing, H. N. Hunter, J. Hagel, H. J. Vogel, *J. Pept. Res.* **2003**, *61*, 219 – 229.
[20] D. J. Schibli, P. M. Hwang, H. J. Vogel, *FEBS Lett.* **1999**, *446*, 213 – 217.
[21] K. Wüthrich, *NMR of Proteins and Nucleic Acids*, Wiley, New York, **1986**.
[22] A. M. Petros, L. Mueller, K. D. Kopple, *Biochemistry* **1990**, *29*, 10041 – 10048.
[23] R. E. Jacobs, S. H. White, *Biochemistry* **1989**, *28*, 3421 – 3437.
[24] J. A. Killian, G. von Heijne, *Trends Biochem. Sci.* **2000**, *25*, 429 – 434.
[25] C. Appelt, F. Eisenmenger, R. Kühne, P. Schmieder, J. A. Söderhäll, *Biophys. J.* **2005**, in press.
[26] W. M. Shafer, F. Hubalek, M. Huang, J. Pohl, *Infect. Immun.* **1996**, *64*, 4842 – 4845.
[27] D. O. Mak, W. W. Webb, *Biophys. J.* **1995**, *69*, 2323 – 2336.
[28] T. Unger, Z. Oren, Y. Shai, *Biochemistry* **2001**, *40*, 6388 – 6397.
[29] A. Rozek, J. P. Powers, C. L. Friedrich, R. E. Hancock, *Biochemistry* **2003**, *42*, 14130 – 14138.
[30] U. Piantini, O. W. Sorensen, R. R. Ernst, *J. Am. Chem. Soc.* **1982**, *104*, 6800 – 6801.
[31] L. Braunschweiler, R. R. Ernst, *J. Magn. Reson.* **1983**, *53*, 521 – 523.
[32] J. Jeener, B. H. Meier, P. Bachmann, R. R. Ernst, *J. Chem. Phys.* **1979**, *71*, 4546 – 4553.
[33] A. A. Bothner-By, R. L. Stephens, J.-M. Lee, C. D. Warren, R. W. Jeanloz, *J. Am. Chem. Soc.* **1984**, *106*, 811 – 813.
[34] C. Appelt, P. Schmieder, unpublished results.
[35] G. W. Vuister, A. Bax, *J. Am. Chem. Soc.* **1993**, *115*, 7772 – 7777.
[36] M. Piotto, V. Saudek, V. Sklenar, *J. Biomol. NMR* **1992**, *2*, 661 – 665.
[37] G. Pintacuda, G. Otting, *J. Am. Chem. Soc.* **2002**, *124*, 372 – 373.
[38] T. D. Goddard, D. G. Kneller, SPARKY 3, University of California, San Francisco, **1998**.
[39] G. Wagner, *Prog. Nucl. Magn. Reson. Spectrosc.* **1990**, *22*, 101 – 139.
[40] D. A. Case, D. A. Pearlman, J. W. Caldwell, T. E. Cheatham III, J. Wang, W. S. Ross, C. Simmerling, T. Darden, K. M. Merz, R. V. Stanton, A. Cheng, J. J. Vincent, M. Crowley, V. Tsui, H. Gohlke, R. Radmer, Y. Duan, J. Pitera, I. Massova, G. L. Seibel, U. C. Singh, P. Weiner, P. A. Kollman, AMBER, University of California, San Francisco, **1999**.
[41] R. Brüschweiler, D. A. Case, *J. Am. Chem. Soc.* **1994**, *116*, 11199 – 11200.
[42] R. Koradi, M. Billeter, K. Wüthrich, *J. Mol. Graphics* **1996**, *14*, 51 – 55.

Received: March 10, 2005
Published online on August 1, 2005

  